

Image Sticking Reduction of Fringe Field Switching LCDs

Daming Xu*, Fenglin Peng*, Haiwei Chen*, Jiamin Yuan*, Shin-Tson Wu*, Ming-Chun Li**,
Seok-Lyul Lee**, Wen-Ching Tsai**

*College of Optics and Photonics, University of Central Florida, Orlando, FL 32816, USA

** AU Optronics Corp., Hsinchu Science Park, Hsinchu 300, Taiwan

Abstract

We propose a kinetic model to characterize the image sticking phenomenon under nonuniform electric field in fringe field switching (FFS) LCDs by taking material properties and device parameters into account. This model agrees well with the experimental results. We investigate the voltage and temperature effects of image sticking based on this model. The image sticking of FFS cells employing positive and negative dielectric anisotropy LCs are compared and the physical mechanisms responsible for the observed differences are explained. In addition, methods for reducing the image sticking are discussed.

Author Keywords

Image sticking; residual DC; fringe field switching.

1. Introduction

Fringe field switching (FFS) LCD [1-3] has been widely used in smart phones and pads because of its wide view, high resolution, and pressure resistance for touch panels. However, image sticking [4-7] and slow response [8-10] still remain to be solved. Image sticking arises from residual DC voltage when a fixed image is displayed for a long period. This phenomenon is very annoying to users and must be minimized or eliminated.

Yasuda *et al.* attributed the generation of residual DC voltage to ion adsorption and desorption and built the first physical model to describe these processes [4]. More recently, Mizusaki *et al.* proposed a more comprehensive kinetic model to describe these processes in homogeneous LC cells [5]. This model assumes that ion adsorption is uniform over the entire interface under uniform longitudinal electric field, thus it does not apply to FFS cells, in which the fringe electric field is not uniform. Hence, we need to develop a new model to describe the generation mechanisms of residual DC voltage in FFS cells.

In this paper, we propose a new kinetic model to characterize the non-uniform adsorption and desorption processes in FFS LCDs. Based on this model, the generation and relaxation of residual DC voltage are studied. Moreover, we compare the residual DC voltage in FFS cells employing positive and negative dielectric anisotropy ($\Delta\epsilon$) LCs and the physical mechanisms behind their differences are explained. In addition, approaches for reducing the image sticking are discussed.

2. Physical Model

The residual DC voltage is caused by offset DC voltage which originates from voltage swing of TFT and flexoelectric effect of LCs. Firstly, a swing in the voltage applied to the LC cell would be generated when the TFT is turned OFF. This voltage swing would impose a DC component on the AC signal. Secondly, the flexoelectric polarization [6, 11] would modify the Freedericksz transition and make the LC distributions different between opposite frames, giving rise to a net offset DC voltage [6].

Initially, the free ions are uniformly distributed in the LC layer. Upon the presence of an offset DC voltage, these free ions

would drift toward and trapped at the interface [4] when a LCD has been driven for a long period, generating a residual DC voltage. In a homogeneous cell, the adsorbed ion density is uniform over the entire adsorption region [5]. In contrast, the scenarios in FFS cells are much more complicated due to the non-uniform electric field, as shown in Fig. 1 is the field profile in a FFS-2/3.5 cell (electrode width $W=2\mu\text{m}$, gap $G=3.5\mu\text{m}$) under 1V applied voltage. As a result, the distribution of adsorbed ions is position-dependent in FFS cells [6].

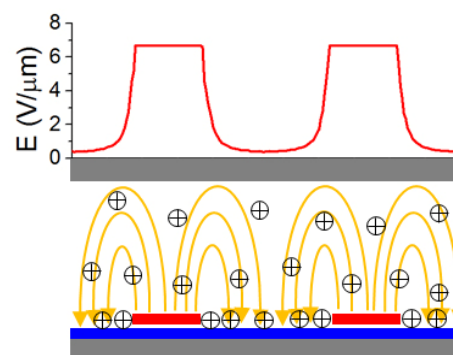


Figure 1. Nonuniform electric field distribution and ion adsorption in a FFS-2/3.5 cell at 1V applied voltage.

In our model, we first assume the adsorbed ion density under a unit electric field ($E_0=1\text{V}/\mu\text{m}$) is $n_0(t)$. The adsorbed ion density increases over time and finally reaches saturation when a unit field is applied. The rate equation of adsorbed ions density is:

$$dn_0(t) / dt = R_a \cdot [n_f - n_0(t)] - R_d \cdot n_0(t), \quad (1)$$

where n_f is the free ion density in the LC layer, R_a and R_d are adsorption and desorption rate constants, respectively. Given the initial condition $n_0(0)=0$, Eq. (1) has following solution:

$$n_0(t) = \frac{R_a \cdot n_f}{R_a + R_d} \left[1 - e^{-(R_a + R_d)t} \right]. \quad (2)$$

Since the density of adsorbed ions is proportional to the field intensity, the position-dependent adsorption can be written as:

$$n(x, t) = E(x)n_0(t) / E_0, \quad (3)$$

where $E(x)$ is the intensity of position-dependent electrical field, as Fig. 1 depicts. Hence, the average adsorbed ion density $n_a(t)$ over the whole adsorption region can be calculated through:

$$n_a(t) = \langle n(x, t) \rangle = \langle E(x) \rangle \cdot n_0(t) / E_0. \quad (4)$$

Here, $\langle E(x) \rangle$ is the average field intensity over the adsorption region. Meanwhile, residual DC voltage V_r is related to n_a by:

$$Q(t) = q \cdot n_a(t) = C_{LC} \cdot V_r(t), \quad (5)$$

where $Q(t)$ is the surface charge and q is a constant ($1.6 \times 10^{-19}\text{C}$). Hence, we obtain following expression for V_r :

$$V_r(t) = \frac{q}{C_{LC}} \cdot \frac{R_a \cdot n_f}{R_a + R_d} \left[1 - e^{-(R_a + R_d)t} \right] \cdot \frac{\langle E(x) \rangle}{E_0}. \quad (6)$$

The exponential term in Eq. (6) implies that V_r would reach a saturation after a sufficiently long period ($t \gg (R_a + R_d)^{-1}$). Thus, to evaluate V_r as a function of time, Eq. (6) can be simplified as:

$$V_r(t) = V_{r,s} \left[1 - e^{-(R_a + R_d)t} \right], \quad (7)$$

where $V_{r,s}$ is the saturated residual DC voltage. Note the second term in Eq. (6) depends on the material properties and needs to be studied via experiments, but the third term is determined by the device parameters and can be calculated through simulations. We simulated $\langle E(x) \rangle$ of FFS cells with different ratios between electrode width (W) and gap (G) under 1V applied voltage using TechWiz LCD and found $\langle E(x) \rangle$ decreases dramatically as the G/W ratio increases. And this trend can be fitted by following equations [12]:

$$\langle E(x) \rangle = \frac{2.979 - 0.369 \cdot G/W}{0.727 + 0.791 \cdot G/W}, \quad (8)$$

Hence, a universal equation has been obtained for V_r of FFS cells by plugging Eq. (8) back into (6). Next, we need to investigate the properties of R_a and R_d through experiments.

3. Experiments

In experiments, we prepared two FFS cells: a positive (p-FFS) and negative (n-FFS) one employing Merck MLC-6686 and -6882, respectively. The material properties are listed in Table II. The cell parameters are: $W=2\mu\text{m}$, $G=3.5\mu\text{m}$, $d\sim 3.2\mu\text{m}$. The ITO electrodes and passivation (Si_3N_4 ; $\epsilon_p=6.5$) are 50nm and 400nm thick, respectively. Both cells are photo-aligned and the photo-alignment material has a $\epsilon=3.9$. During measurement, V_r was evaluated after applying a DC voltage for different time periods, increasing from 10, 20, 30 min, and then to 1, 2, 3, and 4 hours.

TABLE II. Physical properties of two LC mixtures studied ($T = 23^\circ\text{C}$, $\lambda = 633\text{nm}$ and $f = 1\text{ kHz}$).

LC	T_{ni} ($^\circ\text{C}$)	$\epsilon_{//}$	ϵ_{\perp}	$\Delta\epsilon$	Δn
MLC-6686	71.0	14.5	4.5	10.0	0.0969
MLC-6882	69.0	3.6	6.7	-3.1	0.0976

(a) Generation of Residual DC Voltage

Voltage Effect: The voltage effect is studied by measuring transient V_r curves under different voltages V_a , as plotted by the points in Fig. 2. Only the measured data of p-FFS cell are shown here due to limited space, but the n-FFS cell exhibits the same trend: V_r gradually increases over time and finally saturates.

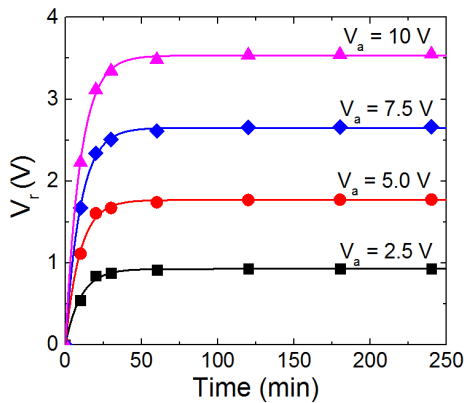


Figure 2. V_r of the p-FFS cell as a function of time under different offset DC voltages at 23°C .

The solid lines in Fig. 2 are the fitting curves using Eq. (7) and well match the measured data. Moreover, we found $V_{r,s}$ is

linearly proportional to V_a from fittings. This is due to more ions are adsorbed to the interface under a higher voltage [5]. Since $V_{r,s}$ determines the severity of image sticking, it is crucial to reduce $V_{r,s}$ by optimizing the material properties.

Temperature Effect: The temperature effect was investigated by applying a 5V offset DC voltage to the p-FFS cell at different temperature. The measured data are plotted as dots in Fig. 3 and the solid lines represent the fitting curves using Eq. (7). Three trends are clearly shown here. Firstly, Eq. (7) fits well with all experimental data, indicating that our model works for different temperature. Secondly, the fitted $V_{r,s}$ is linearly proportional to $1/T$, as the inset plot of Fig. 3 depicts. This is due to more neutral impurities become ionized at an elevated temperature [13], thus giving rise to a higher V_r .

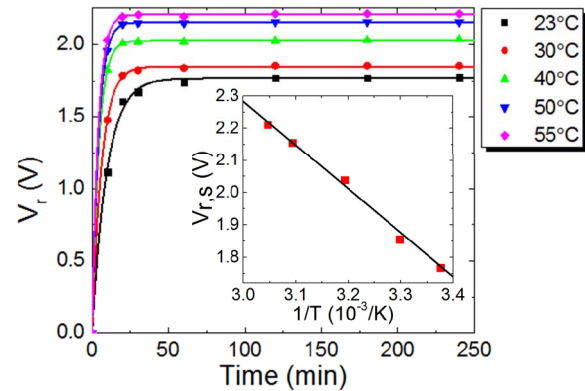


Figure 3. Temperature dependence of V_r . The inset plot shows the fitted $V_{r,s}$ under different temperatures.

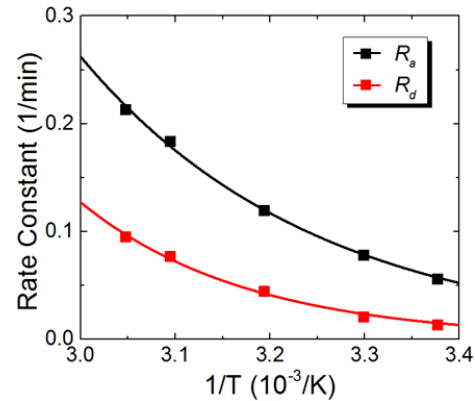


Figure 4. Fitted adsorption and desorption rates (squares) under different temperature. Solid lines represent the fitting curves with Eq. (9).

Moreover, we evaluated R_a and R_d by using Eq. (6), and the fitting results are depicted as squares in Fig. 4. Both R_a and R_d show concave-up curvatures, indicating that they follow the Boltzmann distribution, which arises from the fact that both adsorption and desorption depend on the thermal motion of ions. Therefore, we used the Arrhenius equation to fit R_a and R_d :

$$R = R_0 \exp(-E/kT), \quad (9)$$

where R_0 is a rate constant, E is the activation energy, k is the Boltzmann constant and T is the temperature. The activation energy of adsorption E_a is the energy required to overcome the Coulomb repulsive force between the free ions in the LC layer and the adsorbed ions on the interface. In contrast, the activation energy of

desorption E_d is the energy required for ions to get over the van der Waals interaction between adsorbed ions and alignment layer. Through fittings, we obtained $E_a = 0.487\text{eV}$ and $E_d = 0.348\text{eV}$, on the same order with the ion activation energy between polyimide and 5CB ($\sim 0.5\text{eV}$).

(b) Relaxation of Residual DC Voltage

Upon the removal of the external DC voltage, the adsorbed ions escape from the interface slowly, and this process usually takes several seconds to tens of minutes to finish. In our experiments, the relaxation process of V_r was evaluated by measuring the transient change of V_s , which is a voltage generated by the free charges remained on the electrodes to balance the electric field generated by V_r after removing the applied voltage. Therefore, V_s is complementary to V_r and is related to V_r as:

$$V_s(t) + V_r(t) = V_{s,r}. \quad (10)$$

The solid lines in Fig. 5 show the measured transient V_s change of the p-FFS cell during the relaxation process after applying a 5V DC voltage for 4 hours under different temperature. It clearly shows that two processes are involved in the relaxation curves: a fast one followed by a slow one. This is due to ions with different motilities such as Na^+ , Al^{3+} , Ca^{2+} and K^+ are commonly found in a LC mixture [14, 15]. Hence, there are multiple relaxation processes going on simultaneously and we used a double exponential equation to fit the measured curves:

$$V_s(t) = V_{r,s} \cdot [A \cdot e^{-tR_{d,f}} + (1-A) \cdot e^{-tR_{d,s}}], \quad (11)$$

where $R_{d,f}$ and $R_{d,s}$ denote the rate constant of fast and slow desorption processes, respectively; while A represents the contribution of fast desorption process. The double exponential equation is commonly used to characterize a two mechanism-involved dynamic process [16, 17]. By fitting the measured curves with Eq. (11), we obtained the rates of fast and slow desorption under different temperature, as shown by the dots in the inset plot of Fig. 5. Then we used Eq. (9) to fit these data and found that their temperature dependence follow the Arrhenius equation as well. The fitted activation energies for the fast and slow desorption are 0.271 and 0.475eV, respectively. The difference in activation energy results from the van der Waals interaction between adsorbed ions and interface [4]. It is widely known that the van der Waals force increases as the ion mass gets heavier. Therefore, heavier ions require a higher energy to overcome this force and escape from the interface. Accordingly, the ions with heavier mass are responsible for the slow desorption process, and vice versa.

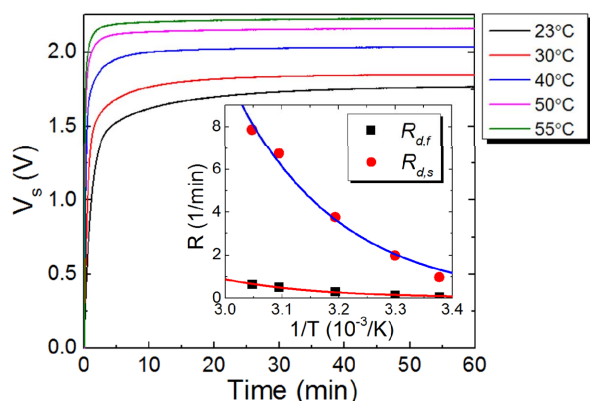


Figure 5. Transient change of V_s at different temperature. (Inset plot: fitted rates for slow (red dots) and fast (black squares) desorption under different temperature. Solid lines represent the fittings with Eq. (9)).

(c) p-FFS vs. n-FFS

Only the results of p-FFS cell were shown above to illustrate the generation mechanisms of residual DC voltage because n-FFS exhibits same trends in voltage and temperature effects. However, there are still some differences between them due to the different LC properties, as outlined below.

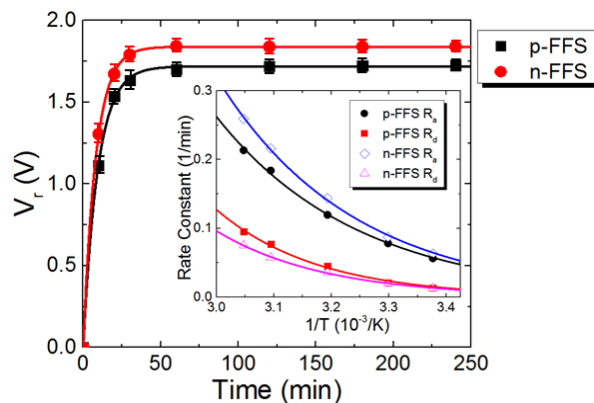


Figure 6. Time-dependent V_r curve of p-FFS and n-FFS. [Inset plot: fitted adsorption and desorption rates of p-FFS and n-FFS. Solid lines are the fittings with Eq. (11)].

Figure 6 shows the measured time-dependent V_r curve of p-FFS and n-FFS at 23°C under an external DC offset voltage of 5V. n-FFS is shown to have a higher V_r than p-FFS, indicating that the image sticking is more severe for n-FFS. Moreover, the time-dependent V_r curve was measured at different temperature and their adsorption and desorption rates also fitted by using the same method described above. The fitting results of p-FFS are shown as solid dots and squares in the inset plot of Fig. 6, while those of n-FFS are represented by open diamonds and triangles. Equation (9) was used to investigate the temperature effect of these fitting results, and the fitted curves are plotted as solid lines in the inset plot of Fig. 6. Through fittings, we found that the adsorption activation energy of n-FFS is lower than that of p-FFS (0.425 vs. 0.487eV), but the desorption activation energy of n-FFS is higher (0.412 vs. 0.348eV). This means in the n-FFS cell it is easier for ions to be adsorbed to the interface but more difficult to desorb, resulting in a more severe image sticking.

Regarding these differences, we believe two reasons need to be considered. Firstly, a negative $\Delta\epsilon$ LC usually employs lateral difluoro compounds, which tend to contain more ionic impurities. Therefore, the free ion density in the negative LC is higher, resulting in a lower VHR [18] and higher residual DC voltage higher for the n-FFS cell. Secondly, the mismatch between dielectric constant is also responsible for the more severe image sticking of n-FFS [19]. According to previous studies, the change in free energy (ΔE) when an ion goes from a medium of dielectric constant ϵ_1 to another with ϵ_2 is [19]:

$$\Delta E = -\frac{Q^2}{8\pi\epsilon_0 a} \left(\frac{1}{\epsilon_1} - \frac{1}{\epsilon_2} \right), \quad (12)$$

where Q is the charge of the ion and a is the ion size. Therefore, it is energetically favorable to transfer ions from the LC layer to alignment layer with a smaller difference in dielectric constant. Here, the dielectric constant of photo-alignment material is $\epsilon = 3.9$, while the average dielectric constant $\langle\epsilon\rangle$ of the positive and negative LCs is 7.83 and 5.67, respectively. The smaller difference between dielectric constant of negative LC and alignment layer implies that ions require a lower energy to be

adsorbed to interface, well matches with our fitting results. Hence, to minimize image sticking, an alignment layer with low ϵ or a LC material with high $\langle\epsilon\rangle$ is helpful.

4. Discussion

In brief, an energy E_a is required to overcome the Coulomb force between ions and climb over the energy barrier in order to make adsorption happen, as Fig. 7 illustrates. On the other hand, weak and strong adsorptions can be differentiated due to the difference in van der Waals interactions. For strongly adsorbed ions, a higher energy $E_{d,s}$ is required to overcome the van der Waals force.

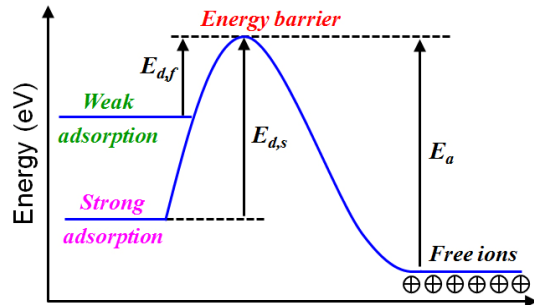


Figure 7. Activation energy diagram for adsorption and desorption of ions.

In order to reduce image sticking, efforts should be made on both material and device sides. From material perspective, an alignment layer with low ϵ or a LC material with high $\langle\epsilon\rangle$ are helpful in obtaining a higher E_a and lower E_d . In addition, making the resistivity of LC close to that of an alignment layer is also significant [7, 18, 19]. On the device side, the choice of LC mode is vital. In terms of display methods, different driving schemes can be employed for different display modes [18].

5. Conclusion

We proposed a kinetic model to characterize the adsorption and desorption under nonuniform electric field in FFS cells. By taking both material properties and device parameters into account, an equation was developed to describe the generation mechanisms of the residual DC voltage. Our model well fits the experimental results and we studied the voltage and temperature effects of the residual DC voltage based on this model. During the adsorption process, an activation energy is required to overcome Coulomb repulsion force between ions in order to adsorb the free ions onto the interface. For the desorption process, ions can be categorized into two groups due to the difference in their mass. These two groups require different desorption activation energies and exhibit different desorption rates. In addition, the residual DC voltages of n-FFS and p-FFS cells are compared. Our results indicate that it is favorable to reduce the difference between the dielectric constants of LC and alignment layer. Our proposed model and experimental evidences are helpful to understand and minimize the image sticking of FFS LCDs.

6. Acknowledgments

The UCF group is indebted to AU Optonics and AFOSR for the financial supports under contract No. FA9550-14-1-0279.

7. References

- [1] S. H. Lee, S. L. Lee, H. Y. Kim, "Electro-optic characteristics and switching principle of a nematic liquid crystal cell controlled by fringe-field switching". *Appl. Phys. Lett.* **73**, 2881-2883 (1998).

- [2] D. H. Kim, Y. J. Lim, D. E. Kim, H. Ren, S. H. Ahn, S. H. Lee, "Past, present, and future of fringe-field switching-liquid crystal display," *Liq. Cryst.* **15**, 99-106 (2014).
- [3] Z. Luo, D. Xu, S. T. Wu, "Emerging quantum-dots-enhanced LCDs" *J. Disp. Technol.* **10**, 526-539 (2014).
- [4] Y. Yasuda, H. Naito, M. Okuda, A. Sugimura, "Observation of adsorption and desorption processes of impurity ions in nematic liquid crystal cells," *Mol. Cryst. Liq. Cryst.* **263**, 559-565 (1995).
- [5] M. Mizusaki, T. Miyashita, T. Uchida, "Behavior of ion affecting image sticking on liquid crystal displays under application of direct current voltage," *J. Appl. Phys.* **108**, 014903 (2010).
- [6] T. Tsuruma, Y. Goto, A. Higashi, M. Watanabe, H. Yamaguchi, T. Tomooka, "Novel image sticking model in the fringe field switching mode based on the flexoelectric effect," *Proc. Eurodisplay* **11**, 19-22 (2011).
- [7] D. H. Kim, Y. J. Lim, D. E. Kim, H. Ren, S. H. Ahn, S. H. Lee, "Investigation on movement of ions in the fringe field switching mode depending on resistivity of alignment layer and dielectric anisotropic sign of liquid crystal," *SID Int. Symp. Dig. Tech. Pap.* **45**, 1421-1423 (2014)
- [8] D. Xu, L. Rao, C. D. Tu, S. T. Wu, "Nematic liquid crystal display with submillisecond grayscale response time," *J. Disp. Technol.* **9**, 67-70 (2013).
- [9] H. Chen, F. Peng, Z. Luo, D. Xu, S. T. Wu, M. C. Li, S. L. Lee, W. C. Tsai, "High performance liquid crystal displays with a low dielectric constant material," *Opt. Mater. Express* **4**, 2262-2273 (2014).
- [10] D. Xu, H. Chen, S. T. Wu, M. C. Li, S. L. Lee, W. C. Tsai, "A fringe field switching liquid crystal display with fast grayscale response time," *J. Disp. Technol.* **11**, 353-359 (2015).
- [11] R. B. Meyer, "Piezoelectric effects in liquid crystals," *Phys. Rev. Lett.* **22**, 918-921 (1969).
- [12] D. Xu, F. Peng, H. Chen, J. Yuan, S. T. Wu, M. C. Li, S. L. Lee, W. C. Tsai, "Image sticking in liquid crystal displays with lateral electric fields," *J. Appl. Phys.* **116**, 193102 (2014).
- [13] S. Murakami, H. Naito, "Charge injection and generation in nematic liquid crystal cells," *Jpn. J. Appl. Phys.* **36**, 773-776 (1997).
- [14] H. Y. Hung, C. W. Lu, C. Y. Lee, C. S. Hsu, Y. Z. Hsieh, "Analysis of metal ion impurities in liquid crystals using high resolution inductively coupled plasma mass spectrometry," *Anal. Methods* **4**, 3631-3637 (2012).
- [15] H. Seiberle, M. Schadt, "LC-conductivity and cell parameters; their influence on twisted nematic and supertwisted nematic liquid crystal displays," *Mol. Cryst. Liq. Cryst.* **239**, 229-244 (1994).
- [16] D. Xu, J. Yan, J. Yuan, F. Peng, Y. Chen, S. T. Wu, "Electro-optic response of polymer-stabilized blue phase liquid crystals," *Appl. Phys. Lett.* **105**, 011119 (2014).
- [17] D. Xu, J. Yuan, M. Schadt, S. T. Wu, "Blue phase liquid crystals stabilized by linear photo-polymerization," *Appl. Phys. Lett.* **105**, 081114 (2014).
- [18] R. Hatsumi, et al. "FFS-mode OS-LCD for reducing eye strain," *J. Soc. Info. Disp.* **21**, 442-450 (2013)
- [19] L. Lu, A. K. Bhowmik, P. J. Bos, "The effect of dielectric constant on ion adsorption in liquid crystal devices," *Liq. Cryst.* **40**, 7-13 (2013).